Published in "Macromolecules 50(14): 5527–5538, 2017"
which should be cited to refer to this work.

Modeling of the Degradation of Poly(ethylene glycol)-*co*-(lactic acid)-dimethacrylate Hydrogels

Vincent E. G. Diederich,[†] Thomas Villiger,[†] Giuseppe Storti,*[,†] and Marco Lattuada*[,‡]

[†]Department of Chemistry and Applied Biosciences, Institute for Chemical and Bioengineering, ETH Zurich, Vladimir-Prelog-Weg 1, CH-8093 Zurich, Switzerland

[‡]Department of Chemistry, University Fribourg, Chemin du Musée 9, CH-1700 Fribourg, Switzerland

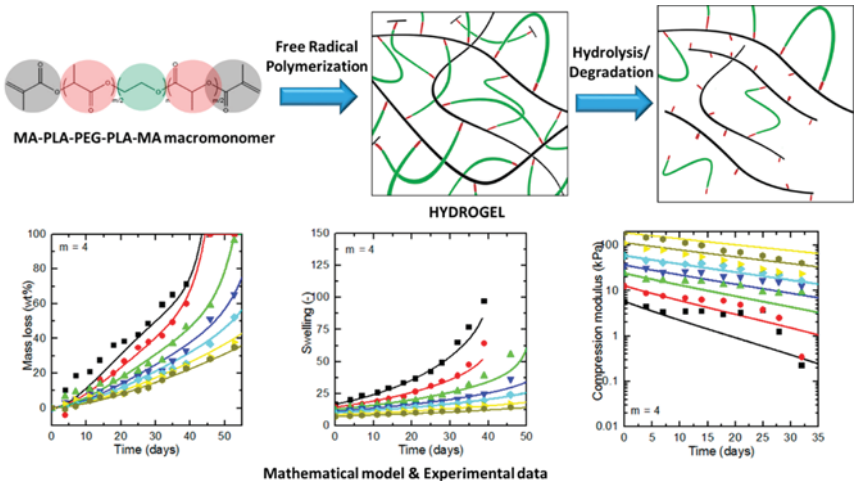

ABSTRACT: Because of their similarity with extracellular matrix, hydrogels are ideal substrates for cell growth. Hydrogels made of synthetic polymers are excellent alternatives to natural ones and offer the key advantage of precisely controllable degradation times. In this work, hydrogels have been prepared from modified poly(ethylene glycol) macromonomers, functionalized on both ends first with a few lactic acid units, and then with methacrylate groups. A library of hydrogels has been prepared using free-radical polymerization of the macromonomers, by changing both the macromonomer concentration and their type, i.e., the number of lactic acid repeating units. The degradation kinetics of these hydrogels, caused by the hydrolysis of the lactic acid units, have been carefully monitored in terms of swelling ratio, mass loss, and Young's modulus. A complete mathematical model, accounting for hydrogel degradation, swelling, and reverse gelation, has been developed and used to predict all the measured quantities until complete disappearance of the gels. The model is capable of accurately predicting the time evolution of all the properties investigated experimentally. To the best of our knowledge, this is the first study where such a systematic comparison between model predictions and experimental data is presented.

INTRODUCTION

Chemically cross-linked polymeric hydrogels are a highly interesting category of materials with a tremendous potential for applications in the area of regenerative medicine,[1] aiming at the repair or the replacement of damaged or nonfunctional tissues. Two-dimensional systems such as polyacrylamide hydrogels[2,3] are very suited for the study of material−cell interactions and offer a great comfort in the experimental characterization (only one focal plane). On the other hand, the development of 3D scaffolds supporting cellular growth, migration, and proliferation[4] is essential to the assessment of potential tissue engineering applications, since cells embedded in a 3D environment behave differently than on a comparable planar surface.[5,6]

The development of such 3D hydrogels is linked to a large number of additional challenges. First of all, the gelation of the biocompatible precursors needs to be performed in the presence of the cells, thus under mild reaction conditions. Then, the hydrogel substrate should degrade in a controllable fashion to allow the formation of functional tissue, requiring both the control of the degradation process and the biocompatibility of the degradation products. Finally, in order to minimize diffusion limitations, the maximum thickness of the hydrogels is usually confined to a few hundred micrometers. The diffusion behavior is of particular relevance, since it is

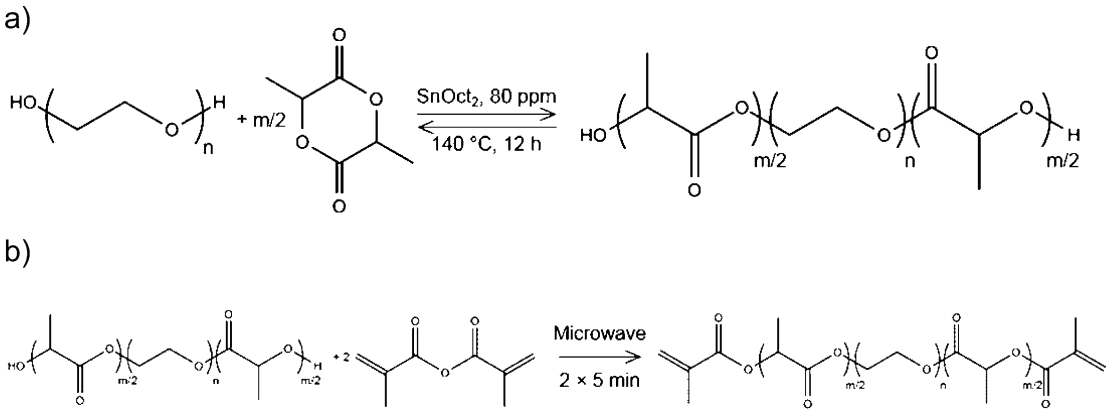

Figure 1. Schematics of the chemical pathway used to synthesize the macromonomers. (a) Ring-opening polymerization of D,L-lactide on PEG. (b) Dimethacrylation of PLA-*b*-PEG-*b*-PLA copolymers with methacrylic anhydride.

responsible for the delivery of nutrients to the cells as well as for the removal of waste and degradation products. Recent efforts focus on overcoming this limitation by introducing vascularization channels into the materials.[7]

As anticipated, in order to encapsulate the cells into a scaffold, mild conditions must be chosen for the gelation to avoid cellular damage. Several techniques have been suggested in the literature to achieve this goal, among which the Michael addition[8] and click reactions[9] seem to be the most promising. However, radical polymerization under controlled conditions such as in UV photopolymerization may also be applied to generate 3D hydrogel matrices around cells, as published by several research groups.[10,11]

A large number of commonly used synthetic macromonomers for the encapsulation of cells are based on poly(ethylene glycol) (PEG) modified with multiple functionalities.[12] Major advantages of PEG are its large solubility and biocompatibility as well as its inhibition of nonspecific protein adhesion, resulting in reduced inflammatory responses. In fact, PEG is frequently conjugated to drug substances increasing their half-life in the human blood.[13]

Among the many PEG-based materials, a popular model system used for the encapsulation of cells in a three-dimensional environment is based on hydrogels prepared from MA-PLA-*b*-PEG-*b*-PLA-MA macromonomers. Through the incorporation of lactic acid (LA) units, the macromonomer becomes degradable via hydrolysis in a time scale useful for potential biomedical applications.[14] Other, less reactive degradable moieties containing ester groups such as glycolic acid or ε-caprolactone have also been reported, leading to reduced degradation rates.[15,16] A large cross-linker is formed by the addition of the methacrylate (MA) groups to the macromonomer. The original, two-step synthesis of this macromonomer, suitable for the preparation of 3D hydrogel networks, was presented by Hubbell et al.[17] The mechanical properties of MA-PLA-*b*-PEG-*b*-PLA-MA hydrogels can be tuned over multiple orders of magnitude in a range of relevance for the investigation of cell−material interactions.[18] The hydrolytic degradation then leads to an opening of the hydrogel structure resulting in a reduction of the hydrogel stiffness. At a critical extent of degradation, the so-called point of reverse gelation, the substrate disintegrates, and all degradation products become soluble.

A considerable amount of modeling work was performed by Metters et al. in order to describe the degradation behavior of MA-PLA-*b*-PEG-*b*-PLA-MA hydrogels in terms of mass loss.[19−22] In their model, the degradation process is dominated by the kinetics of the hydrolytic degradation reaction. As a consequence, all degradation products not linked to the polymethacrylate chains are predicted to immediately leach out of the hydrogel substrate, resulting in a mass loss increase.

This work aims at giving a detailed characterization of the degradation behavior of MA-PLA-*b*-PEG-*b*-PLA-MA hydrogels, accounting for the two-step synthesis of the corresponding macromonomers. First, macromonomers with different numbers of degradable LA units per PEG chain have been produced. Once the synthesized macromonomers were fully characterized, they were used in the production of thick (4 mm) hydrogel slabs of varying compositions (different weight contents of the macromonomer and different numbers of degradable LA units per PEG chain). The hydrolytic degradation process of these hydrogels was measured at physiological conditions in terms of mass loss, swelling ratio, and compressive modulus. Then, a mathematical model has been developed, which, compared to the one developed by Metters et al.,[19] includes a more rigorous description of the degradation kinetics of LA units and of the gel swelling and a more advanced treatment of reverse gelation, based on Flory gelation theory. A thorough validation of the model with a wealth of experimental data has been carried out. The model can accurately predict not only the degradation of the gels but also the time evolutions of their size and mechanical properties.

EXPERIMENTAL SECTION

Materials and Methods. Poly(ethylene glycol) (PEG, M_w = 4000 g mol^{-1}), dichloromethane (DCM, 99.5%), Sn(II) 2-ethylhexanoate ($SnOct_2$, 95%), D,L-lactide (>98%), tetramethylethylenediamine (TEMED, >99.5%), methacrylic anhydride (MAn, 96%), and deuterated chloroform ($CDCl_3$, 99.8%) were obtained from Sigma-Aldrich. Ammonium persulfate (APS, for molecular biology, 98.0%) and toluene (99.7%) were purchased from Fluka. Disodium hydrogen phosphate dodecahydrate (for analysis, 98.5%) and sodium dihydrogen phosphate dihydrate (>98.0%) were purchased from Acros Organics and Merck, respectively. Sodium chloride (NaCl) was obtained from Analar Normapur. Diethyl ether (DEE, >99.5%) and *n*-hexane (>99.5%) were obtained from J.T. Baker.

A conventional microwave oven (MioStar XS, 900 W, Switzerland) was used for the methacrylation reaction. The ^{1}H NMR spectra were recorded on a 500 MHz Bruker spectrometer. The mechanical compression tests were carried out on a Zwick Z020 mechanical testing device with a 200 N load cell. MALDI-TOF spectra were measured on a Bruker Ultra Flex II mass spectrometer. Infrared

transmission spectra were recorded on a Thermo Nicolet Nexus 870 FT-IR spectrometer.

Macromonomer Synthesis. *Synthesis of the PLA-b-PEG-b-PLA Copolymer.* Poly(ethylene glycol)-*co*-poly(lactic acid) (PLA-*b*-PEG-*b*-PLA) block copolymer with different PEG to PLA ratios were synthesized following the description of Hubbell et al.,[17] as schematically shown in Figure 1a. A preliminary experiment charging 4 LA units per PEG chain indicated a conversion of LA units of around 70%, resulting in 2.8 LA units per PEG chain. The target LA content of the PLA-*b*-PEG-*b*-PLA copolymers (4, 8, 12, and 16 LA units per PEG chains, m) was therefore achieved loading 5.6, 11.2, 16.8, and 22.4 units of LA per PEG chain, respectively. In a typical experiment to obtain 4 LA units per PEG chain, PEG (27.8 g, 6.94 mmol) and D,L-lactide (2.80 g, 19.4 mmol) were charged into a dry 100 mL round-bottom flask. After purging the flask with nitrogen for approximately 10 min, the mixture was heated up to 140 °C, and 93.2 μL of 10 wt % solution of $SnOct_2$ in toluene was added. The reaction was stopped after 12 h by removing the oil bath. The product was dissolved in 20 mL of DCM before solidification. The solution was purified twice by reprecipitation in 400 mL of cooled DEE (4 °C) and redissolving it in warm DCM (30 °C). Eventually, the product was dried overnight at 40 °C and 50 mbar and stored in the fridge until use. The preliminary product with 4 LA units per PEG chain was characterized using MALDI-TOF mass spectrometry.

Dimethacrylation of PEG and PLA-b-PEG-b-PLA Copolymer. The dimethacrylation of PEG or PLA-*b*-PEG-*b*-PLA copolymers was performed in a microwave, as schematically shown in Figure 1b. In a typical reaction, PEG (5.00 g, 1.25 mmol) was charged in a 20 mL capped scintillation vial under a nitrogen atmosphere and liquefied in a commercial domestic microwave (250 W) for 1 min. A 5-fold excess of MAn (1.86 mL, 12.5 mmol) was mixed with the molten PEG and placed in the microwave for 5 min at 250 W and then cooled down in an ice bath until solidification of the product started. Subsequent to another 5 min in the microwave at 250 W, the product was cooled down and dissolved in 5 mL of DCM. The product was reprecipitated twice in 80 mL of cooled DEE (4 °C). Eventually, the product was dried overnight at 40 °C and 50 mbar and stored in the fridge until use. The resulting products were characterized with 500 MHz ^{1}H NMR, IR, and MALDI-TOF spectrometry.

Hydrogel Preparation. The radical polymerization of the above-mentioned macromonomers (MA-PEG-MA and MA-PLA-*b*-PEG-*b*-PLA-MA) was carried out in deoxygenized PBS (stripped with nitrogen for at least 20 min). The hydrogel composition was defined through its macromonomer content, w_m, expressed as percentage or fraction; in the latter case:

$$w_m = \frac{\text{mass of macromonomer}}{\text{mass of polymerization solution}} \quad (1)$$

The required amount of macromonomer (e.g., 1.00 g for w_m = 10 wt %) was mixed with PBS (9.00 g), which had been previously stripped with nitrogen, in a 20 mL single neck flask. TEMED (22.4 μL, 150 μmol) was added, and the solution was vigorously stirred under nitrogen injection until the macromonomer had completely dissolved. Subsequent to the addition of a 10 wt % APS solution (102 μL, 50 μmol), the solution was briefly mixed and transferred to a PTFE mold of size 30 × 20 × 4 mm^3. When the polymerization reaction was completed (2 h), the mold was disassembled and the hydrogel was further used for degradation study.

Hydrogel Characterization and Degradation Study. In order to evaluate the degradation behavior of the aforementioned hydrogels, samples with various macromonomer contents (w_m = 6, 7, 8, 9, 10, 11, 12, and 14 wt %) and different amounts of LA units per PEG chain (m = 0, 4, 8, 12, and 16) were prepared. An overview of all the hydrogels prepared for the degradation study is presented in Table 1.

Each of the produced hydrogels was cut into 6 pieces of size 10 × 10 × 4 mm^3 immediately after production. All substrates were weighted to evaluate the hydrogel mass M_H at time t = 0 and stored in 30 mL of PBS at 37 °C. Twice a week, one substrate of each composition was taken out of the oven. The removed sample was weighted to determine its swollen mass. Compression testing was

Table 1. Overview of the Hydrogel Samples Available for the Degradation Study

w_m (wt %)	m = 0	m = 4	m = 8	m = 12	m = 14.7
6	×	×	×	×	
7	×	×	×		
8	×	×	×	×	×
9	×	×	×		
10	×	×	×	×	×
11	×				
12	×	×	×	×	×
14		×	×	×	×

carried out on a Zwick Z020 mechanical testing device (Zwick GmbH & Co. KG, Germany) equipped with a 200 N load cell. The samples were placed on their largest surface between two stainless steel plates. A preload of 0.05 N was used, and the upper plate was moved at a speed of 0.1 mm min^{-1}. The samples were compressed up to a strain of 10%. Following the mechanical testing, the dry mass for the mass loss quantification was measured by drying the hydrogel overnight at 120 °C and 50 mbar. The polymer mass M_P at time t = 0 was obtained from the equation

$$M_P = M_H w_m \quad (2)$$

where M_H is the hydrogel mass at time t = 0. The swelling extent S was evaluated as

$$S = \frac{M_H}{M_{P,d}} \quad (3)$$

where $M_{P,d}$ is the mass of the dry polymer. The compression modulus was evaluated from the slope of the stress−strain curve between 2 and 5% strain. The mass loss L was calculated as

$$L = 1 - \frac{M_{P,d}}{M_P(t=0)} \quad (4)$$

Hydrogel Degradation Model Description. The hydrolytic degradation behavior of MA-PLA-*b*-PEG-*b*-PLA-MA hydrogels was adapted from the scheme described by Metters et al.[19] A schematic of the MA-PLA-*b*-PEG-*b*-PLA-MA hydrogel degradation is shown in Figure 2. After polymerization occurred, the chains are heavily interconnected due to the polymerization of the two methacrylic end groups of the macromonomer (boxes a and d). However, not all the methacrylic groups react during the polymerization as the gelation strongly decreases their accessibility. This leads to a large amount of pendant double bonds and unreacted macromonomers. Since the polymerization is performed in aqueous solution, the degradation of the hydrogel components starts at the moment of the dissolution of the macromonomers. Experimentally, it is therefore of importance to minimize the time lag between the dissolution of the reactants and the polymerization reaction. As the hydrolytic degradation of the labile ester bonds occurs, the hydrogel structure continuously opens up and an increasing amount of degradation products is formed (box b). At a critical extent of cross-linking breakage called "reverse gelation", only branched polymethacrylate chains remain, and the hydrogel structure disassembles (box c).

The first step in building our model was to compare the time scales of diffusion and of degradation reaction. By considering typical values of the diffusion coefficient of water (D = 2.34 × 10^{-5} cm^2/s), sample size (R = 1 cm), and rate constant of degradation (k = 3.8 × 10^{-7} s^{-1}),[14] the ratio of the characteristic times of reaction (t_{reac}) and of diffusion (t_{diff}), calculated as follows:

$$\frac{t_{diff}}{t_{reac}} = \frac{R^2 k}{D} \quad (5)$$

is more than 60, which means that the chemical reaction is the rate-determining step. Under these conditions, it is not necessary to account explicitly for diffusion. Thus, the gel is considered always in

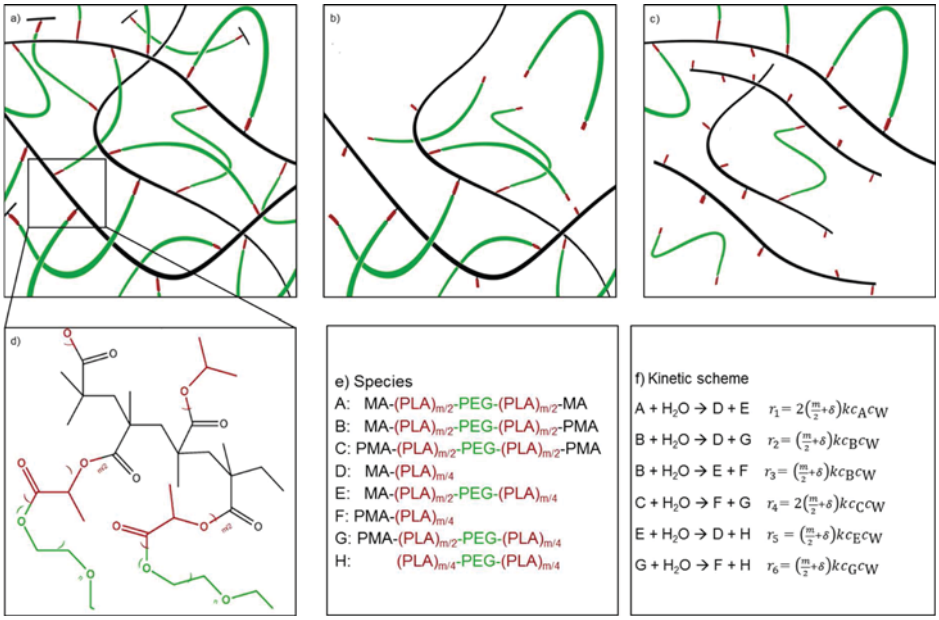

Figure 2. Schematic representation of the hydrolytic hydrogel degradation. The different parts of the macromonomer are color-coded (black: PMA chains; red: PLA chains; green: PEG chains). (a) After production, the hydrogel is a heavily cross-linked polymer network through the polymerization of the methacrylate groups at the end of the macromonomer. (b) Degradation starts the hydrolytic cleavage of the polymethacrylate part from the PEG part. As the degradation reaction proceeds, the hydrogel network gradually weakens. The PEG-based cross-linker fragments diffuse out of the hydrogel structure. (c) Once the degradation has sufficiently advanced, the network falls apart into branched polymethacrylate chains. This point is the so-called reverse gelation. (d) Zoom into the molecular structure of the polymerized hydrogel network. (e, f) Overview of species and kinetic scheme involved in the degradation of the polymer hydrogel. MA and PMA stand for nonpolymerized and polymerized methacrylic groups, respectively.

thermodynamic equilibrium with the surrounding solvent, and the corresponding swelling is evaluated as a function of the degradation extent by the Flory–Rehner theory. The following species will be explicitly considered: the solvent, indicated by the subscript S, the polymer species, indicated by P and expressed in terms of macromonomer repeating units, and the degradation products, indicated by DP. The latter is a lumped species, since it includes all the cross-linker fragments separated from the hydrogel network. Referring to Figure 2, box e, the degradation products include the sum of species A, D, E, and H. Note that A is the unreacted macromonomer; however, since it will diffuse out of the gel instantaneously along with the actual degradation products D, E, and H, it has been included in DP. On the other hand, the polymer species P are further divided into three subgroups. They include the fully cross-linked molecules (C), those connected to the polymer only on one side, but with a long pending chain (species B and G, summed up into the lumped species BG), and those also connected to the polymer on one side but with a short pending chain (F). As the degradation reaches a critical threshold (reverse gelation), the extent of cross-linking becomes not enough to prevent the relative movement of the polymer chains, resulting in complete disintegration of the hydrogel substrate.

Two types of hydrolytic reactions are considered in the overall degradation process. The first one is the reaction involving the hydrolysis of fully cross-linked species, leading to one long and one short pendant chains, while the second one is the overall hydrolytic degradation of long pendant chains, leading to one short pendant chain and to a free degradation product:

$$\text{R1:}\quad \text{C} + \text{H}_2\text{O} \rightarrow \text{BG} + \text{F} \qquad r_1 = 2mkc_{\text{C}}c_{\text{H}_2\text{O}} \tag{6}$$

$$\text{R2:}\quad \text{BG} + \text{H}_2\text{O} \rightarrow \text{F} + \text{DP} \qquad r_2 = mkc_{\text{BG}}c_{\text{H}_2\text{O}} \tag{7}$$

The rate constant k of the PLA hydrolysis is assumed to be identical for both reactions. Furthermore, the reaction rates are proportional to the number of lactic acid units in the chains m. The reactions are assumed to follow second-order kinetics and are proportional to the concentration of polymer chains in the gel as well as to the solvent (i.e., water) concentration. However, the simulation results have also shown that the kinetic constant is a decreasing function of the polymer mass fraction, most probably because high polymer mass fractions reduce the accessibility of degradable chains.

The mass balance equations for the different species belonging to the gel network in terms of molar concentrations are

$$\frac{\mathrm{d}(Vc_{\text{BG}})}{\mathrm{d}t} = 2mkc_{\text{S}}\left(c_{\text{C}} - \frac{1}{2}c_{\text{BG}}\right)V \tag{8}$$

$$\frac{\mathrm{d}(Vc_{\text{F}})}{\mathrm{d}t} = 2mkc_{\text{S}}\left(c_{\text{C}} + \frac{1}{2}c_{\text{BG}}\right)V \tag{9}$$

$$\frac{\mathrm{d}(Vc_{\text{C}})}{\mathrm{d}t} = -2mkc_{\text{S}}c_{\text{C}}V \tag{10}$$

In the above equations, V is the total volume of the hydrogel, which is a function of time. We can now rewrite the equations in terms of volume fractions:

$$\frac{\mathrm{d}(\phi_{\text{BG}})}{\mathrm{d}t} + \frac{\phi_{\text{BG}}}{V}\frac{\mathrm{d}V}{\mathrm{d}t} = 2mk\phi_{\text{S}}\left(\frac{x_{\text{BG}}}{x_{\text{C}}}\phi_{\text{C}} - \frac{1}{2}\phi_{\text{BG}}\right) \tag{11}$$

$$\frac{\mathrm{d}(\phi_{\text{F}})}{\mathrm{d}t} + \frac{\phi_{\text{F}}}{V}\frac{\mathrm{d}V}{\mathrm{d}t} = 2mk\phi_{\text{S}}\left(\frac{x_{\text{F}}}{x_{\text{C}}}\phi_{\text{C}} + \frac{1}{2}\frac{x_{\text{F}}}{x_{\text{BG}}}\phi_{\text{BG}}\right) \tag{12}$$

$$\frac{\mathrm{d}(\phi_{\text{C}})}{\mathrm{d}t} + \frac{\phi_{\text{C}}}{V}\frac{\mathrm{d}V}{\mathrm{d}t} = -2mk\phi_{\text{S}}\phi_{\text{C}} \tag{13}$$

where x_{BG}, x_{F}, and x_{C} are the ratios of the molar volumes of long pending chains, short pending chains, and cross-linked chains, respectively, to the solvent molar volume. Note that the solvent molar volume has been incorporated into the kinetic constant k. Moreover, the following stoichiometric constraints must be fulfilled:

$$\begin{cases} \phi_{BG} + \phi_C + \phi_F = \phi_P \\ \phi_P + \phi_S = 1 \end{cases} \tag{14}$$

The volume fractions of the degradation products and of the solvent are obtained by imposing that they are in thermodynamic equilibrium with the corresponding quantities outside the gel. This leads to the following coupled Flory–Rehner-type equations:[23]

$$\log(\phi_{DP}) + (1 - \phi_{DP}) - x_{DP}\phi_S + \chi\phi_S^2 + \chi\phi_S\phi_{DP}(1 - x_{DP}) + \frac{(\phi_{gel})x_{DP}}{x_C}\left[\left(\frac{V}{V_0}\right)^{2/3} - \frac{1}{2}\right] = \log(\phi_{DP}^{out}) + (1 - \phi_{DP}^{out}) - x_{LP}\phi_S^{out} + \chi x_{DP}(\phi_S^{out})^2 \tag{15}$$

$$\log(\phi_S) + (1 - \phi_S) - \frac{\phi_{DP}}{x_{DP}} + \chi(1 - \phi_S)^2 + \frac{(\phi_{gel})}{x_C}\left[\left(\frac{V}{V_0}\right)^{2/3} - \frac{1}{2}\right] = \log(\phi_S^{out}) + (1 - \phi_S^{out}) - \frac{\phi_{DP}^{out}}{x_{DP}} + \chi(1 - \phi_S^{out})^2 \tag{16}$$

The last terms on the left-hand side of both equations represent the additional constraint to swelling imposed by the presence of cross-linked polymer. It involves the volume fraction of gel polymer in the matrix, ϕ_{gel}, whose evaluation is discussed later in this same section. Additionally, the following stoichiometric condition must be fulfilled:

$$\phi_{DP}^{out} = 1 - \phi_S^{out} \tag{17}$$

In order to solve eqs 15 and 16, it is necessary to complement them with an additional equation, relating the concentration of the degradation products inside and outside the gel. In agreement with the experimental procedure used during the degradation experiments (the gels have been left in contact with a very large quantity of solvent, periodically exchanged with fresh one), it is assumed that the concentration of the degradation products outside the gel undergoes infinite dilution, thus becoming equal to zero. This implies that the only species present outside the gel is the solvent, and according to eq 15, the concentration of degradation products is also zero inside the gel at any time. This is consistent with the fact that the dynamics of the process is dominated by the degradation kinetics. Consequently, when free fragments of macromonomer are generated inside the gel, they instantly diffuse outside it, where there is an infinite reservoir of solvent.

Because of the degradation process, the number of cross-links in the hydrogel will be progressively reduced, leading to a complete disintegration of the gel. In order to account for this effect, called reverse gelation, a more sophisticated approach than the one proposed by Metters et al.[19] has been developed and implemented in this work. It is assumed that because of the gel degradation, the macromonomer units in the gel are in equilibrium with a sol phase, consisting of branched chains no more chemically linked to the gel. As the degradation proceeds, the sol fraction increases, until the number of cross-links is too small to be compatible with the existence of a gel phase and the reverse gelation takes place. To calculate the fraction of sol and gel in the system, a postgel version of the Flory's theory of gelation has been used in a reverse manner.[23] In Flory's gelation theory, explicit expressions for the sol and the gel fractions are provided for systems undergoing polycondensation. In our case, the monomers (or better the macromonomers) consist of a PEG chain, connected on both ends to a certain number of lactic acid units, and finally to two methacrylate groups (one on each side). Therefore, in the formalism developed for polycondensation, each macromonomer is a tetrafunctional unit. The starting concentration of double bonds is known, but upon degradation of the PLA chains, each tetrafunctional unit will be transformed into two difunctional units. If only a single degradation event had occurred for each macromonomer unit, no PEG would be released, but the system would be anyhow transformed from gel into a sol made of linear and branched chains only. Flory's theory leads to an expression for the weight fraction of polymer belonging to the sol and correspondingly for the weight fraction of the gel.

The equations have been taken directly from the paper by Dusek.[24,25] The theory provides the fraction of sol and gel as a function of the fraction of *f*-functional monomer that has reacted. Because of degradation, the initially tetrafunctional macromonomers are progressively transformed into difunctional macromonomers, for which gelation cannot occur. The mass fraction of the sol, w_{sol}, can be found from the following equations:[25]

$$w_{sol} = \left.\frac{\partial g}{\partial s}\right|_{s=1}$$

$$g(s) = s\xi^f - \frac{1}{2}fs\xi^{f-1}[\xi - (1 - \alpha)]$$

$$\xi - \alpha s\xi^{f-1} = (1 - \alpha) \tag{18}$$

where α is the overall conversion of acrylic groups and s a dummy variable. In our case, α is set according to the initial gel conditions, while the functionality of the monomer is not $f = 4$, but rather an average value in between 4 and 2. Such effective functionality can be evaluated as

$$f = 4r + 2(1 - r) = 2r + 2 \tag{19}$$

where r is the ratio between the number of tetra- and difunctional monomer units. This ratio can be readily expressed as a function of the amounts of repeating macromonomer units of the different types, namely as the fraction of *C* units in *P*:

$$r = \frac{c_C}{c_C + c_F + c_{BG}} \tag{20}$$

Finally, this same ratio can be conveniently recast in terms of volume fractions as

$$r = \frac{\phi_C}{\phi_C + \frac{x_C}{x_F}\phi_F + \frac{x_C}{x_{BG}}\phi_{BG}} \tag{21}$$

Using the polymer sol fraction estimated from eq 17, the polymer gel fraction to be used in the Flory–Rehner eq 16 can be evaluated as

$$\phi_{gel} = (\phi_C + \phi_F + \phi_{BG})(1 - w_{sol}) \equiv \phi_P(1 - w_{sol}) \tag{22}$$

The detailed evaluation of the sol fraction, and its time derivatives, necessary to compute the time evolutions of the polymer volume fraction in the system are reported in the Supporting Information.

Finally, the compressive elastic modulus *E* of the hydrogels has been evaluated using the approach outlined by Akalp et al.[26] The relevant equation is the following:

$$E = \frac{RT}{\nu_c\lambda_1}\phi_C\left(\frac{\lambda_1}{S^{1/3}} - \frac{1}{\lambda_1^2}\right) \tag{23}$$

where S is the swelling ratio defined by eq 3, λ_1 is the extent of deformation experienced by the hydrogels during compression, and ν_c is the molar volume of the cross-linker. Since the elastic modulus has been measured by applying a deformation of 10%, $\lambda_1 = 0.1$. Note that according to eq 23 the elastic modulus is proportional to the concentration of cross-links.

Thus, summarizing, the final model is the mixed system of ordinary differential and algebraic eqs 10–17 with all the volume fractions as well as the gel volume as unknowns. The following initial conditions have been used for the differential equations:

$$\begin{cases} \phi_F(t = 0) = 0 \\ \phi_C(t = 0) = \alpha w \\ \phi_{BG}(t = 0) = (1 - \alpha)w \end{cases} \tag{24}$$

The time derivative of the volume, appearing in eqs 11−13, can be expressed through the Flory−Rehner eq 16 and directly substituted in eqs 11−13. This way, a set of three ordinary differential equations is obtained, which has been implemented and solved numerically in Matlab (The Mathworks). All the details about the rearranged model equations are provided in the Supporting Information.

Finally, the model parameter evaluation needs to be discussed. Notably two parameters only have been adjusted by comparison of the model predictions to the experimental results.

The Flory−Huggins parameter has been set equal to the literature value $\chi = 0.45$ for all the simulations.[27]

The degradation rate constant, k, has been found to be a function of the mass fraction of the polymer and, to a lower extent, of the number of lactic acid units. This forced us to consider this quantity as the first adjustable parameter, while assuming the following empirical expression:

$$k = -4.672 \times 10^{-10} w_m^{\,3} + 1.728 \times 10^{-8} w_m^{\,2} - 2.17 \times 10^{-7} w_m + 1.032 \times 10^{-6} \quad \text{for } m < 10$$

$$k = -4.004 \times 10^{-10} w_m^{\,3} + 1.481 \times 10^{-8} w_m^{\,2} - 1.86 \times 10^{-7} w_m + 0.885 \times 10^{-6} \quad \text{for } m > 10 \qquad (25)$$

where w_m is the macromonomer content (in percentage). To better visualize such dependence, a plot of eq 25 is reported in Figure S6 (Supporting Information). Figure S6 shows that the degradation constant changes by about a factor of 3 as the macromonomer constant increases from 6% to 14%. Additionally, as the m value increases above 10, the rate constant is smaller again by about 20%.

The second adjustable parameter is the fraction of methacrylate groups reacted initially in the gel. The list of these values for all the simulated results is reported in Table 2, and all values are in the range from 93 to 98.5%. In general, this value decreases as the mass fraction of polymer increases. The model is quite sensitive to this value, which determines the time when reverse gelation occurs.

Table 2. Value of the Parameter α in Eq 18 for all the Conditions Probed

w_m (wt %)	m = 4	m = 8	m = 12	m = 14.7
6	0.975	0.972	0.99	
7	0.95	0.985		
8	0.945	0.985	0.97	0.98
9	0.935	0.972		
10	0.93	0.965	0.955	0.97
12	0.93	0.97	0.95	0.97
14	0.93	0.97	0.94	0.965

RESULTS AND DISCUSSION

Macromonomer Synthesis. The original PEG was characterized by MALDI-TOF, and the measured spectrum is shown in Figure 3a. On a m/z scale of 3000−5000 g mol^{-1}, the peaks appear to be close to a normal distribution centered around 4050 g mol^{-1}. As expected, the mass difference between two subsequent peaks corresponds to the molecular mass of the ethylene glycol repeating unit, 44 g mol^{-1}. Fitting the distribution of EG repeating units, we ended up with a range of 68−123 EG repeating units, as shown in Figure 3b.

As already mentioned, the synthesis of PLA-*b*-PEG-*b*-PLA copolymer was done through the ring-opening polymerization of D,L-lactide and the stepwise addition of lactic acid units to the two terminal alcohols of the copolymer. Characterization of the preliminary reaction product where four LA units per PEG chain were charged was carried out with MALDI-TOF spectrometry. The result of this analysis can be seen in Figure 4. Part a of this figure shows in black the complex MALDI-TOF spectrum as measured. In color, the fitted spectra of the individual species are overlaid. An enlarged view of the measured spectrum and its fitted counterpart is shown in part b, where the individual species are resolved. It can be seen that species containing up to seven LA units per PEG chain are visible in the spectrum. By fitting the measured spectrum with the calculated spectra of all expected species, it was possible to determine the relative amounts of each species, as subplot c explicitly shows. Integrating over the number of EG repeating units, the distribution of the PLA chain lengths was obtained, as can be seen in part d. One interesting observation is that the distribution of LA units per PEG chain is not at all constrained to even numbers only. This means that there must be a large extent of transesterification reactions of LA units taking place during the synthesis, since no odd numbers of LA units per PEG chain are expected in the ring-opening polymerization of D,L-lactide. From the distribution of the number of LA units per PEG chain, we obtained an average degree of LA polymerization of 2.78, corresponding to a conversion of LA units of 70%. We took this into account for later syntheses of PEG−PLA copolymer by charging an excess of 40% of LA in the ring-opening polymerization (actual and target values have been anticipated in subsection "Hydrogel Characterization and Degradation Study").

A similar characterization was done for the product of the dimethacrylation reaction of PEG, the result of which is shown in Figure S1. A large excess of methacrylic anhydride was charged in order to achieve the highest possible degree of methacrylation per PEG chain (ideally 2), since this is desirable for the hydrogel synthesis. Analysis of the MALDI-TOF spectrum confirmed an average degree of methacrylation of 1.95, with a negligible amount of nonmethacrylated PEG and a small amount of single-methacrylated PEG (4%, as shown in Figure S1c).

Several MA-PLA-*b*-PEG-*b*-PLA-MA macromonomers with different PLA to PEG ratios were then synthesized for the hydrogel degradation study. The resulting products were characterized with FT-IR, as can be seen in Figure S2. Some of the peaks could be assigned to the PEG backbone only (2884, 1342 cm^{-1}, both C−H st sy), while others could be assigned to PEG and PLA (1104, 960 cm^{-1}, C−O−C st as and C−O−C st sy). The presence of methacrylic groups on the MA-PLA-*b*-PEG-*b*-PLA-MA macromonomer was confirmed by the peaks at 1950 (C═CH_2, st), 1717 (C═O, st), 1446 (CH_3−C═C, δ as), and 842 cm^{-1} (C═C(CH_3)-CO, δ oop). Another relevant peak in the characterization of the MA-PLA-*b*-PEG-*b*-PLA-MA macromonomers was located at 1754 cm^{-1}: this peak was assigned to the C═O bond in the LA unit. Indeed, this peak was not seen in the MA-PEG-MA macromonomer (m = 0), and its intensity was increasing with the number of LA units per PEG chain as can be seen in the gray zone in Figure S2, indicating the increasing content of LA units in the macromonomer.

The synthesized MA-PLA-*b*-PEG-*b*-PLA-MA macromonomers were also quantified with ^{1}H NMR. The observed signals and their integrals, interpretation, and multiplicity are reported in Table 3. As expected, the signals at 5.20 ppm (c) and 1.55 ppm (g) only appear in the macromonomers containing LA units. While the other signals are rather constant with changing composition, the signals c and g increase almost linearly with increasing number of LA units per PEG chain charged. From the signals c and g, it was possible to calculate an average

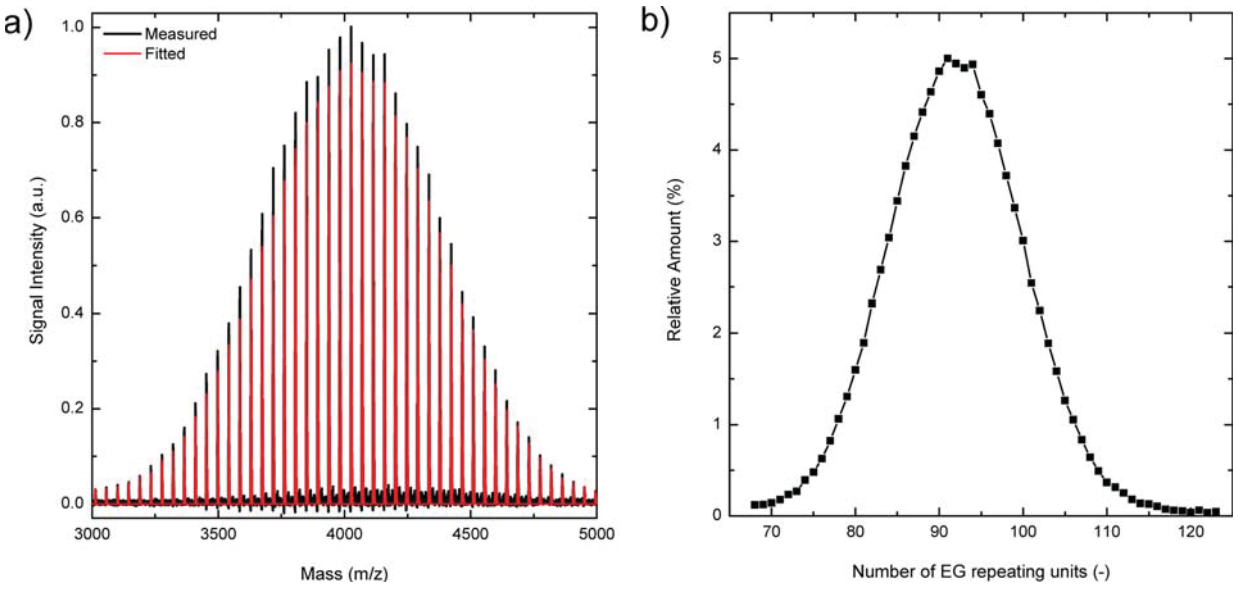

Figure 3. (a) MALDI-TOF spectrum of PEG4000. The black curve corresponds to the measured spectrum, while the red one is the fitted one. (b) Distribution of the EG repeating units in the PEG4000. These data were obtained from the fitting of the MALDI-TOF spectrum shown in (a).

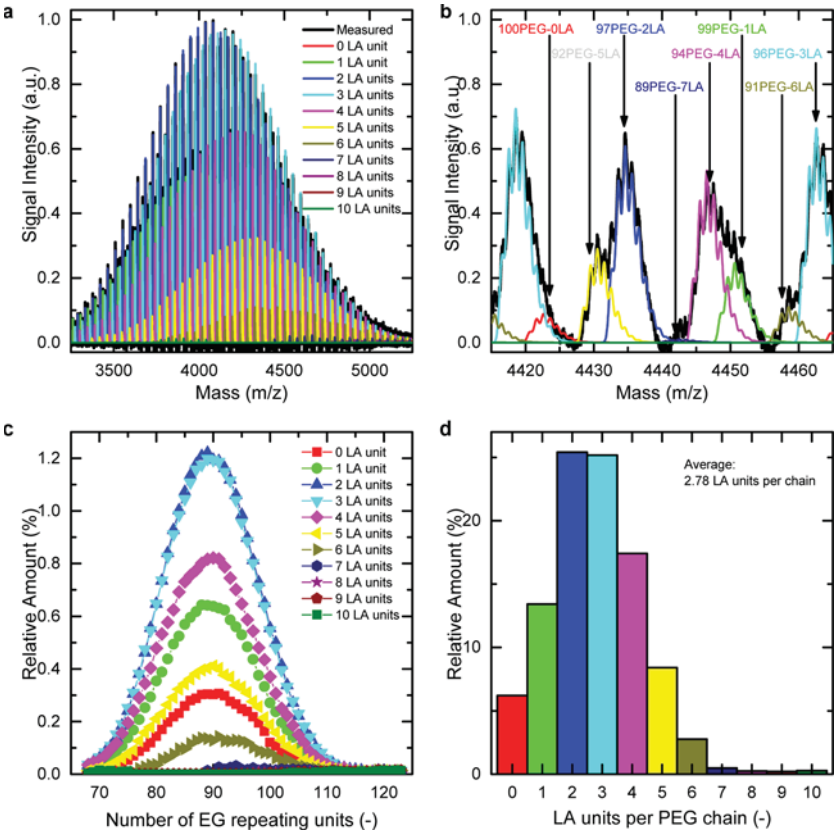

Figure 4. (a) MALDI-TOF signal of the PLA-*b*-PEG-*b*-PLA copolymer obtained by charging 4 LA units per PEG chain. The measured spectrum is shown in black, while the colored spectra correspond to the PLA-*b*-PEG-*b*-PLA copolymers having 1−10 LA units. (b) Zoom into the MALDI-TOF spectrum, which allows the resolution of the different species. (c) Relative amounts of the individual species found in the PLA-*b*-PEG-*b*-PLA product. These results were obtained by fitting the MALDI-TOF spectrum. (d) Distribution of the number of LA units incorporated into each PEG chain. The average of this distribution is 2.78 LA units per PEG chain, resulting in a D,L-lactide conversion of 70%.

number of LA units per PEG chain as a function of the charged amount of D,L-lactide, which is shown in Figure S3a. As can be seen, except for the macromonomer with the highest number of LA units per PEG chain charged, the number of attached LA units per PEG chain increased linearly with the amount of D,L-lactide charged. From the slope of these points, a conversion of 72% was calculated for the D,L-lactide. In a similar way, the average number of MA groups could be determined from the signals at 6.35 ppm (a) and 5.65 ppm (b). It was observed that the dimethacrylation reaction led to a degree of methacrylation

Table 3. Overview of the Measured ^{1}H NMR Signals of PEG-DM and PEG-PLA-DM Copolymers with Different Numbers of LA Units per PEG Chain[a]

Signal	δ (ppm)	Integral size $m = 0$	$m = 4$	$m = 8$	$m = 12$	$m = 14.7$	Multiplicity	Interpretation
a	6.35	2.00	2.00	2.00	1.96	1.98	s	$C=CH_2$
b	5.65	2.09	1.95	2.02	2.06	1.92	s	$C=CH_2$
c	5.20	0.00	3.81	8.09	11.91	14.63	q	CH
d	4.30	4.02	4.28	4.28	4.25	4.12	m	CH_2
e	3.65	360.00	360.00	360.00	360.00	360.00	m	CH_2
f	1.95	5.66	5.74	5.94	6.02	5.93	s	CH_3
g	1.55	0.00	12.29	24.98	36.66	44.03	d	CH_3

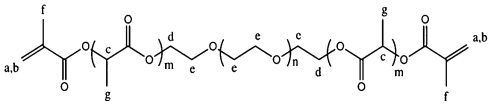

[a]The number of H-atoms corresponds to their total number in one single block copolymer.

of 2 for all the PEG and PLA-*b*-PEG-*b*-PLA copolymers, as visible in Figure S3b.

Hydrogel Synthesis and Degradation. The synthesized hydrogels were transparent and had mechanical properties that strongly depended on the macromonomer content w_m and on the number of LA units per PEG chain m (cf. Figure S4). Similar as for polyacrylamide hydrogels, the hydrogel stiffness increased with increasing macromonomer content. More surprisingly, however, the substrate compression modulus strongly decreased with an increasing number of degradable LA units per PEG chain. This can possibly be imputed to the increasing molecular weight of the macromonomer with increasing number of degradable units.

The degradation behavior of MA-PLA-*b*-PEG-*b*-PLA-MA hydrogels was investigated over durations of up to 55 days in terms of polymer mass loss (Figure 5), hydrogel swelling (Figure 6), and compression modulus (Figure 7). The samples were stored at 37 °C in a large excess of buffer solution.

From the experimental mass loss profiles, several trends and dependencies could be observed:

- As expected, the mass loss strongly depended on the number of LA units per PEG chain m. When increasing the number of degradable units, the mass loss of the hydrogel substrate is strongly accelerated. As an example, one can consider the hydrogels containing 8 wt % of macromonomer after 27 days. The substrate with the nondegrading macromonomer ($m = 0$) exhibited almost negligible mass loss. (In fact, some slow hydrolysis of the ester bonds connecting the methacrylic group to the PEG chains can be observed, but it is considered negligible compared to the degradation rate of the LA units.) At the same time, the mass of the hydrogels containing 4 and 8 LA units per PEG chain diminished by 25.3% and 51.6%, respectively. A further increase in the number of LA units per PEG chain m to 12 or 14.7 resulted in the complete disintegration of the samples in the same lapse of time, corresponding to a mass loss of 100%.
- There is a large dependence of the degradation profile on the macromonomer content w_m. As the macromonomer content increased, the degradation profile was largely slowed down. While 35 days after the start of the hydrolytic degradation, the substrate containing 6 wt % of macromonomer with 4 LA units per PEG chain had already lost most of its mass (65.3%), the mass of corresponding samples containing 8 and 10 wt % of the same macromonomer was reduced by only 37.2% and 22.8%, respectively. When further increasing the macromonomer content to 14 wt %, the mass loss was even more reduced (19.8%). In the model, this trend was empirically accounted for by introducing a dependence of the degradation rate constant on the macromonomer weight fraction w_m.
- For all the degrading substrates, the mass loss abruptly increases to 100% after a certain extent of degradation. This phenomenon, previously called reverse gelation, was observed experimentally by the complete disintegration of the hydrogel substrate. Looking at the hydrogel substrates made from the macromonomer containing 8 LA units per PEG chain, reverse gelation was observed after 20 days for the lowest macromonomer content (w_m = 6 wt %). With increasing macromonomer content, the instant at which reverse gelation occurred increased accordingly (30, 33, 37, 41, 50, and 55 days for w_m = 7, 8, 9, 10, 12, and 14 wt %, respectively).
- Finally, there is also a small extent of degradation visible for the hydrogels composed of the macromonomer with no LA units. This can be explained by the presence of the two ester groups in the macromonomer, which results from the addition of a methacrylic group at each end of

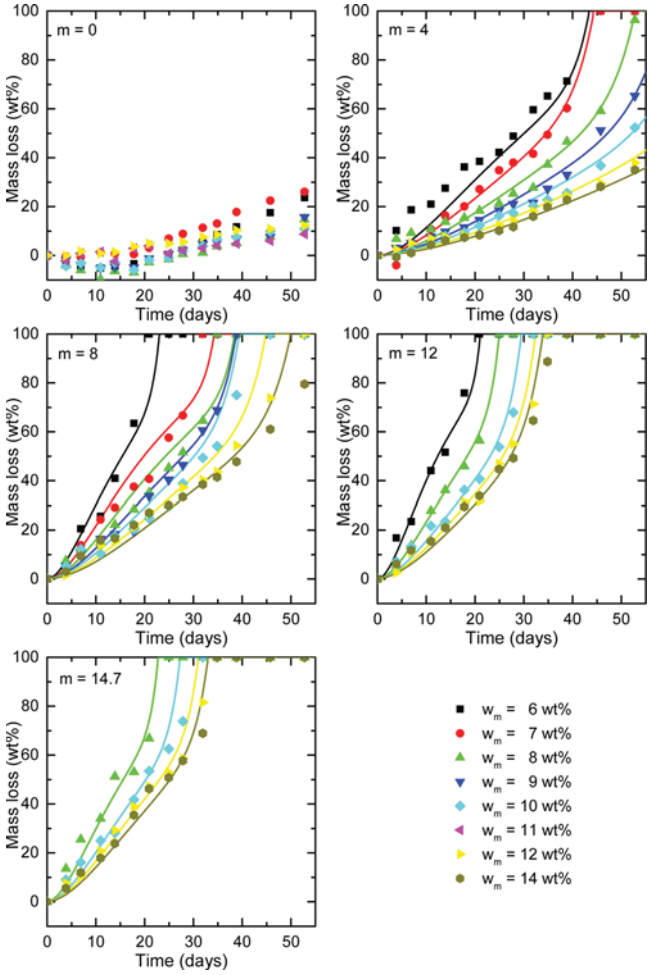

Figure 5. Time evolution of the mass loss for all the samples. The symbols are the experimental data, while the lines are the model predictions.

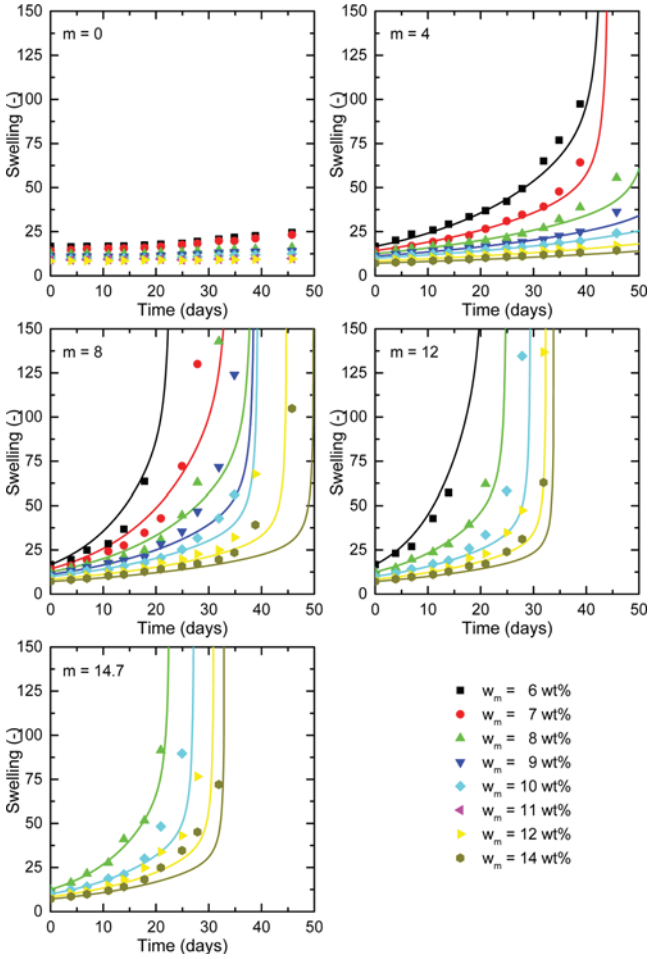

Figure 6. Time evolution of the gel swelling ratio for all the samples. The symbols are the experimental data, while the lines are the model predictions.

the PEG. However, this ester group is much less reactive than the ones from the LA units, and thus, the degradation is significantly slowed down. In addition, it must be mentioned that the negative mass losses observed in the hydrogels with no degradable macromonomer are the result of experimental difficulties to completely remove the water contained from these heavily cross-linked nondegrading hydrogel substrates.

In Figures 5–7, we also added the predictions of the developed mathematical model. As anticipated, the model assumes that diffusion is much faster than degradation, so that hydrogels are constantly in thermodynamic equilibrium with the outer water, assumed to be an infinite reservoir. Additionally, Flory's gelation theory is rigorously introduced to account for the disintegration of the gel caused by the progressive cleavage of the cross-linkers, leading to the so-called reverse gelation phenomenon. Only two parameters have been adapted in the model: the kinetic degradation constant and the initial composition of the gel, i.e., the fraction of reacted acrylic groups.

As already mentioned, the empirical dependence of the kinetic constant k appearing in eqs 6 and 7 on mass fraction of macromonomer and number of lactic acid units m is given by eq 25 (cf. Figure S5; only the first of eq 25 is displayed, the second one being just 20% smaller but with identical trend). The rate constant is decreasing by almost a factor of 3 as the macromonomer mass fraction increases from 6 to 14%, while there is a 20% difference in k at low m vs those at high values. This behavior can be explained in terms of increasing association of the PLA chains in the gel at increasing macromonomer content. Small hydrophobic domains are formed this way, thus decreasing the number of degradable units available for hydrolysis and increasing the time required by water to penetrate them and hydrolyze the chains. This behavior is further enhanced by increasing the number of lactic acid units. The value of the kinetic constant used in the present work was compared to detailed literature data on the hydrolytic degradation of PLA oligomers at different pH conditions.[14] The estimated values used in this work are comprised between 3.5×10^{-7} and 1×10^{-7} s^{-1}, which are not far from those reported in the literature ($\sim 3.8 \times 10^{-7}$ s^{-1}), thus confirming the physical consistency of the model.

The results of the simulations clearly show that the model can describe very satisfactorily the mass loss data for all the gels prepared in this work. Beyond a critical level of degradation, the experimental data indicate the complete disintegration of the gel samples, i.e., the reverse gelation. When considering only the kinetic aspects of the degradation, this situation is established when each polymethacrylate chain is only connected to one other of these chains in average, so that the hydrogel is no longer composed of cross-linked chains, but

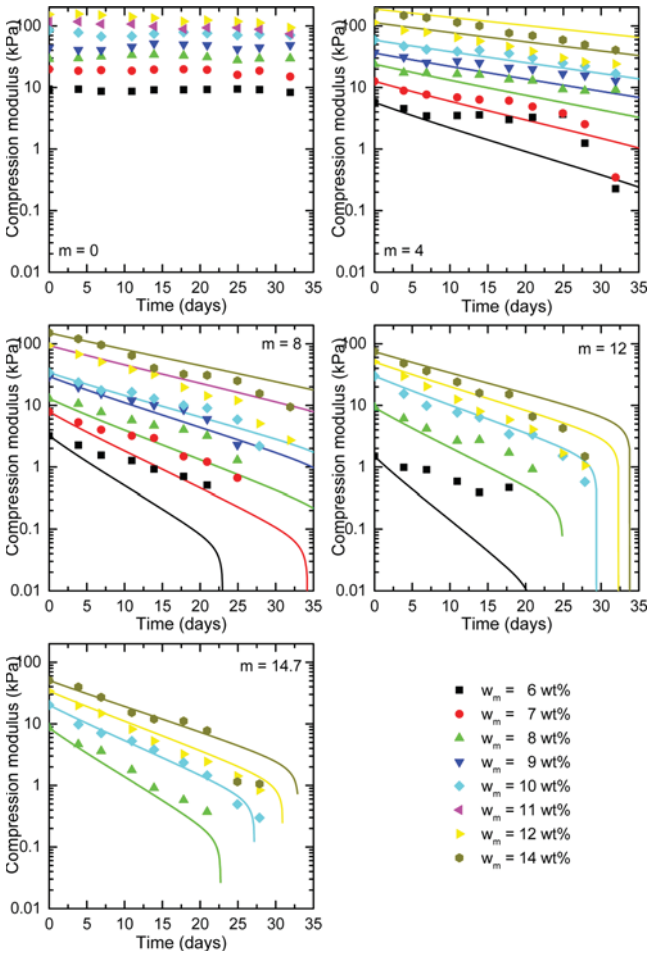

Figure 7. Time evolution of the compression modulus for all the samples. The symbols are the experimental data, while the lines are the model predictions.

rather only of branched and linear chains. At this point, the hydrogel disintegrates and the mass loss suddenly jumps to 100%. In our case, reverse gelation spontaneously occurs when the fraction of sol reaches 100%, which happens when the majority of the cross-linking units is degraded. Differently from what predicted by Metters et al.[19] (who proposed a criterion based on time), the reverse gelation is less abrupt, and it occurs over a finite time interval, as shown by the increase in the sol fraction showcased in Figure S6 for the case m = 8 and w_m = 10%. One can observe that the sol fraction remains negligible over a very long period of time after the beginning of the experiment. On the other hand, the same fraction rapidly increases to 1 when the volume fraction of cross-links drops substantially, as shown in Figure S7 for the same conditions. The sensitivity of the mass loss profile to the value of parameter α is shown in Figure S8. As already mentioned, small variations in the initial conversion of double bonds have a dramatic effect on the time at which reverse gelation occurs, leaving unaltered the initial part of the mass loss profile.

Besides the mass loss behavior of the degrading substrates, we also measured the extent of swelling for durations of up to 50 days. The swelling ratio was calculated as the ratio of the mass of the hydrogel substrate and its dry mass at a given time. The obtained results are shown in Figure 6. Similar trends as for the mass loss can be observed. First of all, the value of swelling initially increases in time as the hydrogel structure becomes weaker. This process is autoaccelerating as the slope of the swelling curves continuously increases with time. Not surprisingly, this phenomenon is even further accelerated with increasing the number of degradable LA units per PEG chain, m. At a certain extent of swelling, the hydrogel completely disintegrates and reverse gelation occurs, resulting in infinite swelling. When changing the macromonomer content w_m in the hydrogel, the substrates start with a smaller swelling value and the denser polymer network contributes to a deceleration of the swelling profiles. The model predicts equally satisfactorily also the swelling kinetics of the gels, as shown in Figure 6, without introducing any additional adjustable parameter. One should however note that the model tends to overestimate the time when the swelling ratio increases before reverse gelation occurs. The model predicts this time to be identical to that for which mass loss experiences its rapid surge, while experimentally it looks like the swelling ratio starts to increase more rapidly at earlier time points.

A further method for characterizing the degrading substrates was to measure their compression modulus. The change in time of the compressive modulus is shown in Figure 7. Again, all trends observed in the mechanical properties are consistent with the mass loss and the swelling profiles. As the number of LA units per PEG chain m is increased or as the macromonomer content w_m is reduced, the overall degradation is accelerated. One should note that the model predictions have been determined by using the initially measured value of compressive modulus as starting point and then by using the Flory–Rehner theory to compute the relative change in modulus. In this case, the model predictions are slightly less satisfactory but still overall consistent with the trends observed in the experimental results. It is also possible to note that when reverse gelation occurs, the elastic modulus values drops to zero, as it is physically expected.

CONCLUSIONS

This work presents extensive experimental data and modeling of hydrolytic degradation of PEG-based hydrogels, which have already successfully been used for the 3D culture of cells in the literature.[10,11] First, the synthesis of the MA-PLA-*b*-PEG-*b*-PLA-MA macromonomers was performed according to the procedure proposed by Hubbell et al.[17] through the stepwise addition of LA units followed by methacrylic groups. The ring-opening metathesis polymerization of D,L-lactide resulted in an average conversion of 72%. In this way, macromonomers with different numbers of LA repeat units (m = 0, 4, 8, 12, and 14.7) per PEG chain were prepared. The analysis of the PLA-*b*-PEG-*b*-PLA copolymers by MALDI-TOF revealed the strong extent of transesterification, since many macromonomers with an odd number of LA repeating units were detected. The methacrylation reaction was carried out through the addition of a large excess of methacrylic anhydride, resulting in an almost perfect degree of methacrylation.

In the second part of the work, the large difunctional macromonomers were polymerized to generate heavily cross-linked hydrogels at different macromonomer contents and different numbers of degradable ester bonds per PEG chain. The degradation behavior of the resulting substrates was measured at 37 °C in PBS in terms of polymer mass loss, swelling extent, and compression modulus. The trends observed in all three types of measurements were consistent, and an increase in mass loss simultaneously resulted in an increase in the extent of swelling as well as a reduction of the

compression modulus. With increasing duration of the degradation, increasing mass loss profiles were observed in all prepared substrates. However, the rate of mass loss was strongly dependent on mainly two factors: first, as expected, increasing the reactivity of the PLA chain through the increase in the number of degradable units in it significantly accelerated the mass loss behavior. In addition, a rise in the macromonomer content in the hydrogel resulted in a deceleration of the degradation velocity. Experimentally, the phenomenon of reverse gelation was observed: at this point, the substrate entirely disintegrated and all its degradation products became soluble in the buffer solution.

Next to the large extent of experimental data presented, we developed a quite general model including explicit time evolution of the swelling of the gels, degradation kinetics, and reverse gelation. Diffusion limitations were estimated to be completely negligible because the kinetics is controlled by the degradation process. The model is based on a system of three ODEs, coupled with a few algebraic equations, and contains only two adjustable parameters: (i) the kinetic rate constant of the degradation reaction as a function of the system composition, eq 25, for which a physical explanation was proposed; (ii) the initial conversion of acrylic bonds, which affects the time where reverse gelation occurs. An entirely new theory for reverse gelation was finally proposed, based on the Flory's gelation theory. The model provides very good agreement over the entire set of experimental data. The results obtained, and in particular the developed mathematical model, will help designing more effective hydrogels with precisely tuned degradation properties.

■ ASSOCIATED CONTENT

Supporting Information

The Supporting Information is available free of charge on the ACS Publications website at DOI: 10.1021/acs.macromol.7b00902.

Figures S1−S8 and eqs 1−7 (PDF)

■ AUTHOR INFORMATION

Corresponding Authors

*E-mail: giuseppe.storti@chem.ethz.ch.
*E-mail: marco.lattuada@unifr.ch.

ORCID

Marco Lattuada: 0000-0001-7058-9509

Notes

The authors declare no competing financial interest.

■ ACKNOWLEDGMENTS

We acknowledge financial support from the Bonizzi-Theler Foundation and the Stipendienfonds der Schweizerischen Chemischen Industrie (SSCI). M.L. acknowledges financial support from the Swiss National Science Foundation (SNSF), with Grant PP00P2_159258, as well as to the NCCR program Bioinspired materials. G.S. acknowledges financial support from the Swiss National Science Foundation with Grant 200021.153403/1.

■ REFERENCES

(1) Fedorovich, N. E.; Alblas, J.; de Wijn, J. R.; Hennink, W. E.; Verbout, A. J.; Dhert, W. J. A. Hydrogels as extracellular matrices for skeletal tissue engineering: state-of-the-art and novel application in organ printing. *Tissue Eng.* **2007**, *13* (8), 1905−1925.

(2) Sharma, R. I.; Snedeker, J. G. Biochemical and biomechanical gradients for directed bone marrow stromal cell differentiation toward tendon and bone. *Biomaterials* **2010**, *31* (30), 7695−7704.

(3) Lo, C. M.; Wang, H. B.; Dembo, M.; Wang, Y. L. Cell movement is guided by the rigidity of the substrate. *Biophys. J.* **2000**, *79* (1), 144−152.

(4) Nuttelman, C. R.; Rice, M. A.; Rydholm, A. E.; Salinas, C. N.; Shah, D. N.; Anseth, K. S. Macromolecular monomers for the synthesis of hydrogel niches and their application in cell encapsulation and tissue engineering. *Prog. Polym. Sci.* **2008**, *33* (2), 167−179.

(5) Cukierman, E.; Pankov, R.; Stevens, D. R.; Yamada, K. M. Taking cell-matrix adhesions to the third dimension. *Science* **2001**, *294* (5547), 1708−1712.

(6) Ko, D. Y.; Shinde, U. P.; Yeon, B.; Jeong, B. Recent progress of in situ formed gels for biomedical applications. *Prog. Polym. Sci.* **2013**, *38* (3−4), 672−701.

(7) Schimek, K.; Busek, M.; Brincker, S.; Groth, B.; Hoffmann, S.; Lauster, R.; Lindner, G.; Lorenz, A.; Menzel, U.; Sonntag, F.; Walles, H.; Marx, U.; Horland, R. Integrating biological vasculature into a multi-organ-chip microsystem. *Lab Chip* **2013**, *13* (18), 3588−3598.

(8) Lutolf, M. P.; Hubbell, J. A. Synthesis and physicochemical characterization of end-linked poly(ethylene glycol)-co-peptide hydrogels formed by Michael-type addition. *Biomacromolecules* **2003**, *4* (3), 713−722.

(9) DeForest, C. A.; Anseth, K. S. Cytocompatible click-based hydrogels with dynamically tunable properties through orthogonal photoconjugation and photocleavage reactions. *Nat. Chem.* **2011**, *3* (12), 925−931.

(10) Marklein, R. A.; Burdick, J. A. Spatially controlled hydrogel mechanics to modulate stem cell interactions. *Soft Matter* **2010**, *6* (1), 136−143.

(11) Chatterjee, K.; Lin-Gibson, S.; Wallace, W. E.; Parekh, S. H.; Lee, Y. J.; Cicerone, M. T.; Young, M. F.; Simon, C. G., Jr. The effect of 3D hydrogel scaffold modulus on osteoblast differentiation and mineralization revealed by combinatorial screening. *Biomaterials* **2010**, *31* (19), 5051−5062.

(12) Liu, S. Q.; Tay, R.; Khan, M.; Ee, P. L. R.; Hedrick, J. L.; Yang, Y. Y. Synthetic hydrogels for controlled stem cell differentiation. *Soft Matter* **2010**, *6* (1), 67−81.

(13) Pfister, D.; Morbidelli, M. Process for protein PEGylation. *J. Controlled Release* **2014**, *180*, 134−149.

(14) Lazzari, S.; Codari, R.; Storti, G.; Morbidelli, M.; Moscatelli, D. Modeling the pH-dependent PLA oligomer degradation kinetics. *Polym. Degrad. Stab.* **2014**, *110*, 80−90.

(15) Colombo, C.; Dragoni, L.; Gatti, S.; Pesce, R. M.; Rooney, T. R.; Mavroudakis, E.; Ferrari, R.; Moscatelli, D. Tunable Degradation Behavior of PEGylated Polyester-Based Nanoparticles Obtained Through Emulsion Free Radical Polymerization. *Ind. Eng. Chem. Res.* **2014**, *53* (22), 9128−9135.

(16) Lin, G.; Cosimbescu, L.; Karin, N. J.; Tarasevich, B. J. Injectable and thermosensitive PLGA-g-PEG hydrogels containing hydroxyapatite: preparation, characterization and in vitro release behavior. *Biomed. Mater.* **2012**, *7* (2), 024107.

(17) Sawhney, A. S.; Pathak, C. P.; Hubbell, J. A. Bioerodible Hydrogels Based on Photopolymerized Poly(Ethylene Glycol)-Co-Poly(Alpha-Hydroxy Acid) Diacrylate Macromers. *Macromolecules* **1993**, *26* (4), 581−587.

(18) Engler, A.; Bacakova, L.; Newman, C.; Hategan, A.; Griffin, M.; Discher, D. Substrate compliance versus ligand density in cell on gel responses. *Biophys. J.* **2004**, *86* (1), 617−628.

(19) Metters, A. T.; Bowman, C. N.; Anseth, K. S. A statistical kinetic model for the bulk degradation of PLA-b-PEG-b-PLA hydrogel networks. *J. Phys. Chem. B* **2000**, *104* (30), 7043−7049.

(20) Metters, A. T.; Anseth, K. S.; Bowman, C. N. A statistical kinetic model for the bulk degradation of PLA-b-PEG-b-PLA hydrogel networks: Incorporating network non-idealities. *J. Phys. Chem. B* **2001**, *105* (34), 8069−8076.

(21) Metters, A. T.; Anseth, K. S.; Bowman, C. N. Fundamental studies of a novel, biodegradable PEG-b-PLA hydrogel. *Polymer* **2000**, *41* (11), 3993−4004.
(22) Metters, A. T.; Bowman, C. N.; Anseth, K. S. Verification of scaling laws for degrading PLA-b-PEG-b-PLA hydrogels. *AIChE J.* **2001**, *47* (6), 1432−1437.
(23) Flory, P. J. *Principles of Polymer Chemistry*; Cornell University Press: Ithaca, NY, 1953.
(24) Dusek, K. Correspondence between the Theory of Branching-Processes and the Kinetic-Theory for Random Crosslinking in the Post-Gel Stage. *Polym. Bull.* **1979**, *1* (8), 523−528.
(25) Ziff, R. M.; Stell, G. Kinetics of Polymer Gelation. *J. Chem. Phys.* **1980**, *73* (7), 3492−3499.
(26) Akalp, U.; Chu, S.; Skaalure, S. C.; Bryant, S. J.; Doostan, A.; Vernerey, F. J. Determination of the polymer-solvent interaction parameter for PEG hydrogels in water: Application of a self learning algorithm. *Polymer* **2015**, *66*, 135−147.
(27) Eliassi, A.; Modarress, H.; Mansoori, G. A. Measurement of activity of water in aqueous poly(ethylene glycol) solutions (Effect of excess volume on the Flory-Huggins chi-parameter). *J. Chem. Eng. Data* **1999**, *44* (1), 52−55.